Formation of bimetallic core-shell nanowires along vortices in superfluid He nanodroplets

Philipp Thaler,[1] Alexander Volk,[1] Florian Lackner,[1] Johannes Steurer,[1] Daniel Knez,[2] Werner Grogger,[2]
Ferdinand Hofer,[2] and Wolfgang E. Ernst[1],*

[1]*Institute of Experimental Physics, TU Graz, Petersgasse 16, A-8010 Graz, Austria*
[2]*Institute for Electron Microscopy and Nanoanalysis & Graz Centre for Electron Microscopy, TU Graz,*
Steyrergasse 17, A-8010 Graz, Austria

We report on the formation of one-dimensional Au/Ag core-shell nanostructures in superfluid helium nanodroplets (He_N) and their subsequent surface deposition under soft landing conditions. In vortex charged He_N, dopant atoms and clusters prefer to agglomerate along vortex cores, which serve as personal cryo-templates for each nanowire. A sequential pickup scheme enables the fabrication of Au/Ag structures with either Au as core and Ag as shell or vice versa. The core-shell structure is in both cases shown by energy-dispersive x-ray spectroscopy (EDX) in a scanning transmission electron microscope (STEM). The inherent spatial resolution and element sensitivity of this method allows a direct observation of the two different phases. High resolution STEM studies elucidate morphological details of the Au/Ag nanostructures and, together with the EDX analysis, indicate that the nanowires are formed in a multicenter aggregation process.

The recent years have seen a tremendous growth of interest in one-dimensional nanostructures, accompanied with intriguing applications in various fields of research [1]. Especially carbon nanotubes and core-shell structures offer great prospects for nanophysics because of their tailorable properties, with new emerging applications ranging from nanoelectronics [2,3] to material science [1] and catalysis [4]. Helium nanodroplets (He_N) entered the stage of one-dimensional nanoparticles only very recently in a seminal work that demonstrated the formation of elongated Ag structures along quantized vortices and their subsequent surface deposition [5]. In contrast to He_N experiments, which allow a defined formation of isolated nanowires in single droplets, experiments in bulk superfluid helium have already been used for the preparation of nanowire bundles [6–9]. In this article we show that the He_N approach can be exploited for the deliberate formation of one-dimensional core-shell nanostructures with predefined core and shell materials. The exceptional doping capabilities and high cooling rates provided by He_N suggest that this approach offers a novel route to a large variety of new material combinations which may exhibit revolutionary properties.

He_N provide a gentle, low temperature environment (0.37 K) for the preparation of tailored molecules and clusters [10,11]. Their outstanding features enabled fascinating experiments [10–12] leading to new insights into various phenomena in physics, such as the study of superfluidity on a microscopic scale [13–15], the observation of the superfluid phase in hydrogen [16], or the spectroscopic investigation of homo- and heteronuclear high-spin alkali dimers and trimers [17–19]. A new emerging branch in He_N isolation utilizes the method for the production and subsequent surface deposition of nanoclusters [20,21], nowadays routinely done with various atomic and molecular building blocks [12,22–24]. Their sizes can be well controlled by adjusting the pickup conditions and the mean helium droplet size, where the latter is dictated by nozzle temperature (T_0) and stagnation pressure (p_0) [10,11].

Previously, the approach has been used for the preparation of small core-shell clusters with rare gas atoms or gas molecules as shells [25–27]. It has been shown that clusters formed in helium droplets can be deposited on surfaces [20] under soft-landing conditions [28,29], which allows a subsequent analysis by transmission electron microscopy (TEM) [21,28,30,31]. Very recently, the existence of vortices in He_N has been demonstrated [5]. Thereby it has been exploited that dopant atoms and clusters (Ag) prefer to reside at vortex sites, which can be observed upon surface deposition in the form of elongated wire structures in TEM studies. This experiment attracted strong interest and the method has recently been introduced for the vortex-assisted preparation of ultrathin one-dimensional nanostructures [32,33]. The production of bimetallic core-shell clusters has been envisaged [20,21,31], but the actual structure of these clusters has so far not been determined unambiguously by element sensitive and spatially resolved methods. Possible configurations for bimetallic nanoparticles are alloyed states or separated phases as for example in core-shell particles or Janus particles (i.e., configurations where each of the phases forms one hemisphere of the particle) [34].

In this article we explore if a sequential pickup scheme leads to the formation of core-shell particles, as has been speculated in previous publications [20,21,31]. Our experiments yield bimetallic nanowires with core-shell structures, where the center of the particle is rich in the element which is picked up first and the outer region of the particle is rich in the element which is picked up second. As materials we chose Ag and Au as they are miscible and exhibit very similar lattice parameters. With conventional techniques it would be hard to create separated phases on a nanometer length scale with these elements.

The helium droplet apparatus used in the experiments was designed for the production of very large droplets, details will be published elsewhere. In short, the setup consists of three vacuum chambers, separated by skimmers, with subsequently decreasing background pressure. In the first chamber He droplets are produced via supersonic expansion of precooled high purity (99.9999%) helium into vacuum

---

*wolfgang.ernst@tugraz.at

through a nozzle (diameter 5 μm) which is cooled by a closed cycle refrigerator ($T_{\min} < 4$ K). In the second chamber multiple modularly designed evaporation cells, which consist of resistively heated crucibles containing the desired dopant, can be placed. The maximum crucible temperature of 2000 K allows doping the droplets with a large variety of materials and the interchangeability of the cells enables choosing arbitrary doping sequences. Finally, the beam of doped droplets enters a UHV chamber in which the created nanoparticles can be analyzed and deposited onto surfaces, e.g., commercial TEM substrates.

The produced samples were analyzed *ex situ* using a probe-corrected FEI Titan[3] 60-300 high-resolution scanning transmission electron microscope (HR-STEM) equipped with a Super-X detector for energy-dispersive x-ray spectroscopy (EDXS) and a Gatan Quantum energy filter for electron energy loss spectroscopy (EELS). In order to avoid sample damage, a low dose condition with a beam current of 50 pA and a low dwell time were used. Furthermore, subpixel scanning was activated during the acquisition of spectrum images (SIs) in order to spread the dose over the whole pixel size.

With the experimental setup, droplets consisting of 10^3 to $>10^{10}$ He atoms (diameter 4 nm to >1 μm) can be created. To produce clusters in He$_N$, large droplet sizes are required because the pickup of dopant atoms and the subsequent cluster formation results in a release of energy, which leads to the evaporation of helium atoms and consequently a shrinking of the droplet. For metal dopants, a broad size range, going from monomers up to clusters consisting of several 10^5 atoms, can be covered. Besides the helium droplet diameter, the size of the clusters obtained in an experiment strongly depends on the vapor pressure in the pickup region, which is controlled by the temperature of the evaporation cells. For experiments with Ag and Au, oven temperatures close to the respective melting points (1235 and 1337 K) were used.

The tunability of the He$_N$ allows the controlled growth of nanowires in single droplets in terms of length and composition. This is in contrast to experiments in bulk superfluid helium where always bundles of nanowires are produced and their length is determined by the physical constraints of the superfluid [6–8]. In agreement with the results presented in Refs. [5] and [33] we find exclusively spherical particles at $T_0 > 7$ K and $p_0 = 20$ bar. In the experiments presented in this article we used $T_0 = 6$ K and $p_0 = 20$ bar, which leads to an exponential droplet size distribution with an initial mean droplet size of $\bar{N} \approx 3 \times 10^8$ He atoms (diameter ≈ 300 nm) [35]. This expansion condition is slightly beyond the onset of the vortex regime [5,33] and well suited for the production of linear one-dimensional nanoparticles with only a small number of branched structures. The temperatures of the Ag and Au evaporation cells were adjusted by measuring the dopant mass flow, which is transported by the beam, with a quartz crystal microbalance as well as by monitoring the He-beam attenuation, caused by the evaporation of He atoms off the droplet upon pickup, with a quadrupole mass spectrometer set to 4 amu. In the experiments, the temperatures were chosen to yield an equal amount of Ag and Au atoms in each droplet and to evaporate about 50% of all He atoms upon pickup. This doping level is a good tradeoff between creating large clusters and preserving the He$_N$ beam.
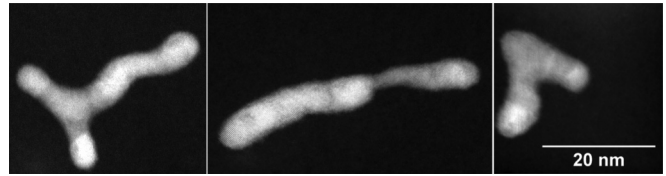

FIG. 1. Representative STEM HAADF images of branched, straight, and kinked wires with Au core and Ag shell on a 3 nm thick amorphous carbon substrate.

Under this condition, STEM investigations of the produced nanoparticles show wire structures with an average length of about 30 nm and an average diameter of approximately 7 nm. The majority of the observed nanowires exhibits a linear shape, but also kinked and branched particles were found on the substrate. High angle annular dark field (HAADF) images of some of the observed shapes are shown in Fig. 1. The observation of branched structures is attributed to the presence of multiple vortices in large He$_N$ [5]. Considering the low surface coverage, it can be excluded that these structures originate from overlapping linear nanoparticles created in different droplets.

In the experiments, two different pickup sequences were applied. In the first, the Au source was placed in the upstream and Ag source in the downstream position (Au/Ag, Fig. 2), and in the second the arrangement was reversed (Ag/Au, Fig. 3). The images in Figs. 2 and 3 show detailed studies of linear nanowires, including bright field (BF) and HAADF images [(a) and (b), respectively] as well as elemental maps recorded with EDXS. In both figures, the color map in (e) is based on the EDX data shown in (c) and (d) of the respective figure, with red corresponding to Au and green corresponding to Ag. To obtain the SI [(c) and (d)], each pixel was illuminated for about 2 s and the EDX data were smoothed via a spatial convolution filter with a size of 3×3 pixels [36].

In Fig. 2, where Au was doped first to the He$_N$, a Au-rich core and a Ag-rich shell region can be seen. Figure 2(d), which depicts exclusively Au atoms, shows that the core of this particle is continuous. In Fig. 2(c), which depicts exclusively Ag atoms, the nanowire exhibits a slightly larger diameter than in Fig. 2(d), indicating the Ag-shell structure. The same characteristic was found when imaging the Ag fraction with
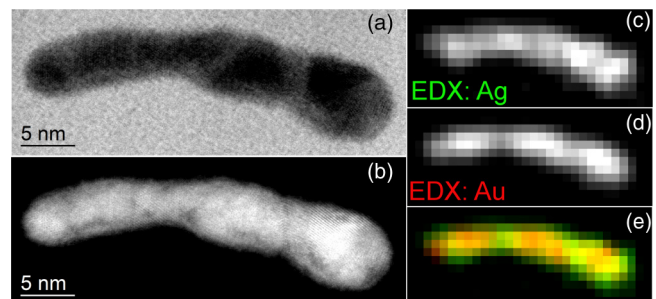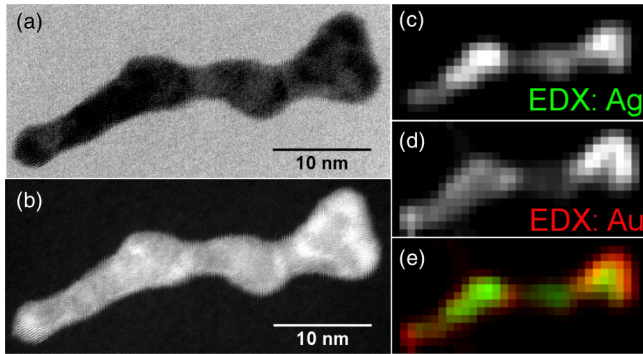

FIG. 2. (Color online) STEM images of a nanowire with Au as core and Ag as shell: BF image (a), HAADF image (b), EDX SI Ag (Ag L_α line) (c), EDX spectrum image (SI) Au (Au L_α line) (d), and colored overlay image of the Ag and Au EDX SI (e).

FIG. 3. (Color online) STEM images of a nanowire with Ag as core and Au as shell: BF image (a), HAADF image (b), EDX SI Ag (Ag L_α line) (c), EDX SI Au (Au M_α line) (d), and colored overlay image of the Ag and Au EDX SI (e).

EELS (electron energy loss spectroscopy), as depicted in Fig. 4. In contrast, in Fig. 3, where the pickup sequence was reversed, a Ag-rich core and a Au-rich shell region are present. This demonstrates that the core-shell sequence is determined by the pickup sequence. In both cases, the cross section of the wires does not stay constant over their entire length. Constrictions between bulging parts of the nanowires and alternations in the EDX intensity along the wire (e) indicate that they grew in a multicenter growth process [37], starting from single spherical particles which subsequently aligned and connected along the vortices. The existence of domain boundaries between the bulging parts of the nanowires are apparent in high resolution images (Fig. 5) and corroborate the multicenter growth scenario. A possible explanation for the nonuniform distribution of the core material over the length of the wires is a slower than expected capture and connection process in the vortices. Our results suggest that the wire formation of the first material is not complete as the droplets enter the second pickup cell. Either clusters of the first material are captured but not yet connected inside the vortices as they are covered by the second material, or spherical pure
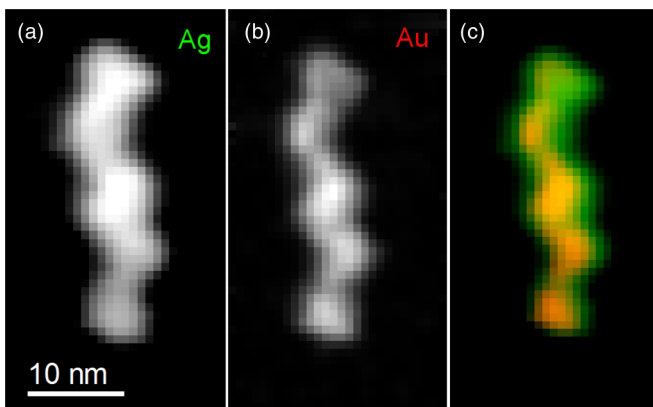

FIG. 4. (Color online) STEM images of a nanowire with Au as core and Ag as shell: EELS SI Ag (a), EDX SI Au (Au L_α line) (b), and colored overlay image of the simultaneously obtained Ag EELS SI and Au EDX SI (c). The winding shape of the wire is at least partly caused by the sample drift (several minutes illumination time).
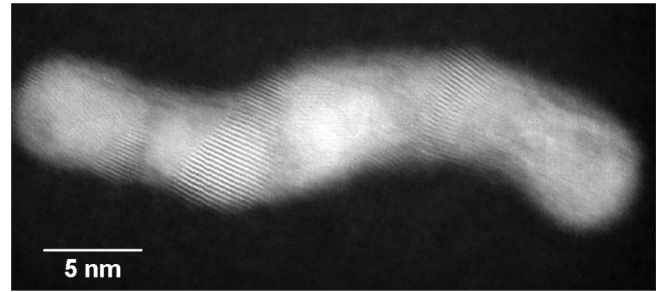

FIG. 5. HAADF image, showing domain boundaries in a Au-core and Ag-shell nanowire.

clusters of both materials and/or spherical core-shell clusters get pinned to the vortices not until after the second pickup cell. During cluster and wire growth, the low temperature environment combined with the high cooling rate leads to a fast dissipation of the binding energy of the shell material and thus prevents the two materials from alloying. The low velocity of the He$_N$ as well as the cushioning effect of the evaporating helium atoms in the moment of impact lead to ultrasoft landing conditions which enable the survival of the core-shell structure upon deposition.

In general, the interpretation of BF (a) and HAADF (b) images of samples with varying thickness (also in Ref. [33]) is difficult. In that case, the contrast seen in these images can originate from the different thickness of the sample and not only from the different atomic number of the constituents (Z contrast). In contrast, the element sensitive EDX provides detailed information about the element distribution in the nanoparticles [(c)–(e)].

The interpretation of x-ray photoelectron spectroscopy (XPS) results, as presented for Au-Ni nanoparticles in Ref. [21], is even more problematic in terms of characterizing their internal structure. While the absence of a pronounced core-level shift in XPS indicates that Au and Ni do not alloy in these particles, the method cannot clarify the spatial distribution of different phases and thus cannot be taken as evidence for a core-shell structure. Furthermore, XPS investigations always cover relatively large areas and thereby average over a large number of nanoparticles. Only element- *and* spatially-sensitive methods give an insight into the actual distribution of the constituents in a single particle for this kind of samples.

For the transfer from our experimental setup to the microscope, the samples were shortly exposed to ambient conditions (exposure time <5 min). Measurements with different exposure times (up to a few hours) showed no change in any of the particle characteristics. When using the low dose condition (beam current of 50 pA) in the STEM, the samples were stable under illumination by the electron beam, otherwise the EDX investigations, which usually take up to 30 min to image a single particle, would not be possible. In general, the particles seem to be very robust. Note that, in terms of long time stability, it has been reported that initially alloyed Au-Ag clusters of similar size can change their structure and form Janus particles within a time span of two years [38].

In summary, we demonstrated that core-shell Au/Ag and Ag/Au nanowires can be formed by using vortices in He$_N$

as cryo-templates. By utilizing two pickup schemes, which differ in the sequence of the Au and Ag evaporation sources, it was shown that the resulting core and shell constituents are determined by the order of the pickup ovens and that their sequence can be reversed. Evidence for the respective structures is based on EDX, which provides element sensitive and spatially resolved images of these nanowires for the first time. Furthermore, the element distribution obtained by EDX gives insight into the formation process of the wires. Variations in the EDX-intensity of the different phases along the wires as well as the existence of domain boundaries and constrictions between the spherical sections of the wires indicate that they are formed in a multicenter growth process, starting from single spherical particles which subsequently aligned and connected along the vortices. In contrast to conventional methods, the helium droplet approach does not require chemical agents in order to dictate the shape and the sequence of the layers. Additionally, the fabricated structures can be deposited on virtually any substrate that can be implemented into a UHV apparatus. The low velocity of the He_N as well as the cushioning effect of the evaporating helium in the moment of impact ensure soft landing conditions, thus preserving the initial structure upon deposition.

Increasing the distance between the pickup cells may lead to more pronounced core-shell structures with a continuous core and may even allow the creation of a core-multishell system. The exceptional doping abilities of He_N allow to envisage the controlled formation of nanoparticles made from gaseous, liquid, or solid building blocks. The preservation of the core-shell structure upon deposition would allow the passivation of reactive core-species by a nonreactive shell layer, in order to conserve the core for subsequent investigations [39].

The formation of tailored metal clusters inside He_N may open new prospects in helium droplet research, which could lead to a new research branch. In surface enhanced Raman scattering (SERS) experiments [40] single-molecule sensitivity has been reported [41]. We propose that the enhancement of the Raman effect by nanoparticles may allow *in situ* Raman spectroscopy of single molecules doped to He_N that contain a nanocluster. Tailored Au/Ag core-shell nanostructures can enable a tuning of plasmon resonances (which have been observed in Ag_n-He_N [37]), in order to increase the SERS enhancement factors, which may lead to intriguing new insights in fundamental physics, helium nanodroplet science, as well as SERS and material science.

---

[1] L. Cademartiri and G. A. Ozin, Adv. Mater. **21**, 1013 (2009).

[2] W. Lu and C. M. Lieber, Nat. Mater. **6**, 841 (2007).

[3] C. M. Lieber, MRS Bull. **28**, 486 (2011).

[4] *Nanocatalysis*, edited by U. Heiz and U. Landman (Springer-Verlag, Berlin, 2007).

[5] L. F. Gomez, E. Loginov, and A. F. Vilesov, Phys. Rev. Lett. **108**, 155302 (2012).

[6] P. Moroshkin, V. Lebedev, B. Grobety, C. Neururer, E. B. Gordon, and A. Weis, Europhys. Lett. **90**, 34002 (2010).

[7] V. Lebedev, P. Moroshkin, B. Grobety, E. Gordon, and A. Weis, J. Low Temp. Phys. **165**, 166 (2011).

[8] E. B. Gordon, A. V. Karabulin, V. I. Matyushenko, V. D. Sizov, and I. I. Khodos, Appl. Phys. Lett. **101**, 052605 (2012).

[9] E. B. Gordon, A. V. Karabulin, A. A. Morozov, V. I. Matyushenko, V. D. Sizov, and I. I. Khodos, J. Phys. Chem. Lett. **5**, 1072 (2014).

[10] C. Callegari and W. E. Ernst, in *Handbook of High Resolution Spectroscopy*, Vol. 3, edited by F. Merkt and M. Quack (John Wiley & Sons, Chichester, 2011), pp. 1551–1594.

[11] J. P. Toennies and A. F. Vilesov, Angew. Chem. Int. Ed. **43**, 2622 (2004).

[12] J. Tiggesbäumker and F. Stienkemeier, Phys. Chem. Chem. Phys. **9**, 4748 (2007).

[13] S. Grebenev, J. P. Toennies, and A. F. Vilesov, Science **279**, 2083 (1998).

[14] A. R. W. McKellar, Y. Xu, and W. Jäger, Phys. Rev. Lett. **97**, 183401 (2006).

[15] J. Tang, Y. Xu, A. R. W. McKellar, and W. Jäger, Science **297**, 2030 (2002).

[16] S. Grebenev, B. Sartakov, J. P. Toennies, and A. F. Vilesov, Science **289**, 1532 (2000).

[17] J. Higgins, C. Callegari, J. Reho, F. Stienkemeier, W. E. Ernst, K. K. Lehmann, M. Gutowski, and G. Scoles, Science **273**, 629 (1996).

[18] J. Higgins, W. E. Ernst, C. Callegari, J. Reho, K. K. Lehmann, G. Scoles, and M. Gutowski, Phys. Rev. Lett. **77**, 4532 (1996).

[19] J. Nagl, G. Auböck, A. W. Hauser, O. Allard, C. Callegari, and W. E. Ernst, Phys. Rev. Lett. **100**, 063001 (2008).

[20] V. Mozhayskiy, M. N. Slipchenko, V. K. Adamchuk, and A. F. Vilesov, J. Chem. Phys. **127**, 094701 (2007).

[21] A. Boatwright, C. Feng, D. Spence, E. Latimer, C. Binns, A. M. Ellis, and S. Yang, Faraday Discuss. **162**, 113 (2013).

[22] S. Denifl, F. Zappa, I. Mähr, J. Lecointre, M. Probst, T. D. Märk, and P. Scheier, Phys. Rev. Lett. **97**, 043201 (2006).

[23] M. Theisen, F. Lackner, and W. E. Ernst, J. Phys. Chem. A **115**, 7005 (2011).

[24] C. P. Schulz, P. Claas, D. Schumacher, and F. Stienkemeier, Phys. Rev. Lett. **92**, 013401 (2004).

[25] J. Liu, B. Shepperson, A. M. Ellis, and S. Yang, Phys. Chem. Chem. Phys. **13**, 13920 (2011).

[26] W. K. Lewis, B. E. Applegate, J. Sztáray, B. Sztáray, T. Baer, R. J. Bemish, and R. E. Miller, J. Am. Chem. Soc. **126**, 11283 (2004).

[27] E. Loginov, L. F. Gomez, and A. F. Vilesov, J. Phys. Chem. A **117**, 11774 (2013).

[28] E. Loginov, L. F. Gomez, and A. F. Vilesov, J. Phys. Chem. A **115**, 7199 (2011).

[29] P. Thaler, A. Volk, M. Ratschek, M. Koch, and W. E. Ernst, J. Chem. Phys. **140**, 044326 (2014).

[30] A. Volk, P. Thaler, M. Koch, E. Fisslthaler, W. Grogger, and W. E. Ernst, J. Chem. Phys. **138**, 214312 (2013).

[31] S. Yang, A. M. Ellis, D. Spence, C. Feng, A. Boatwright, E. Latimer, and C. Binns, Nanoscale **5**, 11545 (2013).

[32] D. Spence, E. Latimer, C. Feng, A. Boatwright, A. M. Ellis, and S. Yang, Phys. Chem. Chem. Phys. **16**, 6903 (2014).

[33] E. Latimer, D. Spence, C. Feng, A. Boatwright, A. M. Ellis, and S. Yang, Nano Lett. **14**, 2902 (2014).

[34] I. Parsina and F. Baletto, J. Phys. Chem. C **114**, 1504 (2010).

[35] L. F. Gomez, E. Loginov, R. Sliter, and A. F. Vilesov, J. Chem. Phys. **135**, 154201 (2011).

[36] B. D. Forbes, A. J. D'Alfonso, R. E. A. Williams, R. Srinivasan, H. L. Fraser, D. W. McComb, B. Freitag, D. O. Klenov, and L. J. Allen, Phys. Rev. B **86**, 024108 (2012).

[37] E. Loginov, L. F. Gomez, N. Chiang, A. Halder, N. Guggemos, V. V. Kresin, and A. F. Vilesov, Phys. Rev. Lett. **106**, 233401 (2011).

[38] D. Belić, R. L. Chantry, Z. Y. Li, and S. A. Brown, Appl. Phys. Lett. **99**, 171914 (2011).

[39] S. B. Emery, K. B. Rider, and C. M. Lindsay, Propellants, Explosives, Pyrotechnics **39**, 161 (2014).

[40] K. Kneipp, M. Moskovits, and H. Kneipp, Phys. Today **60**(11), 40 (2007).

[41] S. Nie and S. R. Emory, Science **275**, 1102 (1997).